

Confinement factor and carrier recombination of InGaAsP/InP quantum well lasers

E. M. T. Salman^{a,*}, M. R. Jobayr^b, H. K. Hassun^a

^a*Department of Physics, College of Education for Pure Science (Ibn-AL-Haitham)/University of Baghdad, Iraq*

^b*Dept. Radiology Technology/College of Health and Medical Technology / Middle Technical University (MTU), Iraq*

Low-dimensional materials have attracted significant attention in developing and enhancing the performance of quantum well lasers due to their extraordinary unique properties. The optical confinement factor is one of the most effective parameters for evaluating the optimal performance of a semiconductor laser diode when used to measure the optical gain and current threshold. The optical confinement factor and the radiative recombination of single quantum wells (SQW) and multi-quantum wells (MQW) for InGaAsP/InP have been theoretically studied using both radiative and Auger coefficients. Quantum well width, barrier width, and number of quantum wells were all looked at to see how these things changed the optical confinement factor and radiative and non-radiative recombination coefficients for multi-quantum well structures. It was found that the optical confinement factor increases with an increase in the number of wells. The largest value of the optical confinement factor was determined when the number of wells was five at any width. The optical confinement coefficient was 0.23, 0.216, and 0.203 for the number of wells (3, 4, and 5) and well width (27, 19.5, and 15) nm, respectively. In addition, the radiative recombination coefficient increases with the width of the quantum well after 5 nm, and it is much bigger than that of its bulk counterparts.

(Received April 12, 2022; Accepted August 17, 2022)

Keywords: Quantum well laser, Optical confinement factor, Carrier recombination, Semiconductor laser, InGaAsP/InP.

1. Introduction

Low-dimensional materials, due to their exceptional characteristics, have attracted increasing interest in various fields. These extraordinary and remarkable properties play an important role in theories of the evolution of quantum well (QW) structures in general, and the development of QW lasers in particular [1, 2]. The trend towards nano-dimension laser materials such as quantum wells, quantum wires, and quantum dots is the most prominent feature of the evolution of these materials [3-5]. Much attention has been paid to the quantum well, and scientists and experts are still seeking to benefit from these structures, particularly QW lasers. One of the most prominent characteristics is the significant increase in the optical gain, which is offset by a very low current density. Several factors, such as the optical confinement factor and the width of the active region, play a prominent role in amplifying electromagnetic waves by stimulating emission [6-8]. The optical confinement factor is one of the most effective parameters for evaluating optimal performance in a semiconductor laser diode that is used to measure current threshold and optical gain. The active region plays an essential role in determining the laser confinement factor, where the confinement factor is low when the active area is thin [9, 10]. To determine and predict laser behavior, it is necessary to evaluate the optical confinement factor for any laser material. On the other hand, the efficiency of the device in generating the laser increases with the increase in the carrier's radioactive recombination. The recombination process, as specified by the Fermi-Dirac population function, happens in the density of states of distinct structures and is the polar opposite of the generation process [11]. The generation process is the

* Corresponding author: ibtisam.m.t@ihcoedu.uobaghdad.edu.iq
<https://doi.org/10.15251/JOR.2022.184.617>

process of transferring the electron from the conduction band to the valence band, and this leads to the generation of an electron-hole. As for the recombination process, it is the process of returning the electron from the conduction band to the valence band [12], emitting the energy difference in the form of photons. There are two forms of recombination: radioactive recombination and non-radioactive recombination. Understanding semiconductor physics in optoelectronic devices like light emitting diodes and solar cells relies heavily on non-radioactive recombination [13]. When the carriers in the conduction band recombine with carriers in the valence band, non-radiative recombination occurs, meaning no light is released. This process leads to an increase in the current required to produce the laser [14]. Non-radiative recombination reduces the efficiency of the device by reducing the range of photons generated by the carriers. When current is introduced into a semiconductor laser, an electron-hole pair generates a photon, which causes the required recombination in the active region. However, there are additional processes that produce carrier loss, which contributes to the threshold and degrades device performance. The main non-radiative processes include recombination at Auger recombination and defects [15]. In Auger recombination, the energy generated by electron-hole recombination is absorbed by another electron, which is then stimulated to a higher energy state. The excited electron must lose energy in order to reach thermal equilibrium. The phonons, or grid vibrations, will absorb the energy that has been lost. When a defect is present, however, recombination occurs owing to the capture of carriers in states formed by local defects, where the carriers are nonradiatively recombined. Because of the lower energy steps and the confined character of the defect, phonon emission becomes more plausible [13].

In this paper, the effects of the optical confinement factor, Radiative recombination coefficient, and Auger coefficient of the InGaAsP/InP quantum well laser are investigated to show that it is possible to achieve an interaction between these parameters to enhance the gain coefficient of this photonic crystal. Moreover, we implement a realistic data set for comparisons to demonstrate that the proposed quantum well structures provide a better fit than single quantum well structures, including the determination of the emitted wavelength region. Therefore, this work can enrich the potential applications of quantum well lasers, such as optical communications and transmission systems.

2. Theoretical Model

2.1. Confinement factor

The overlap between the laser's optical-mode pattern and gain region (i.e. quantum well) is defined by a confinement factor (Γ), which is calculated using: [16]

$$\Gamma = \frac{\int_{-w/2}^{w/2} E_0^2(x) dx}{\int_{-\infty}^{+\infty} E_0^2(x) dx} \quad (1)$$

where is the intensity of the electrical field for the first transverse mode generation in the active region. The first transverse mode (TE_0) departing the active layer has an electrical field intensity ($E_0(z)$). The following equation is almost analytical for computing the optical confinement factor (Γ) in a single quantum well:[17]

$$\Gamma^{SQW} \cong \frac{\tau^2}{\tau^2 + 2} \quad (2)$$

where τ is the normalized thickness of active layer given by: $\tau = 2\pi \left(\frac{w}{\lambda}\right) \sqrt{(n_w^2 - n_c^2)}$, where, w is the active region width, λ is the wavelength of the emitted photon and n_c, n_w are the refractive indexes of cladding and active region respectively. When utilizing heterostructures, the refractive index can vary dramatically. As a result, the multi-quantum well's optical confinement factor may be represented as [18, 19]:

$$\Gamma^{MQW} = \Gamma^{SQW} \frac{N_w w}{L} \quad (3)$$

where L is the active layer's average thickness, and w and N_w are the well width and number of wells, respectively. Recognizing the importance of the numbers of wells and barrier layers number, N_B , in the computation of L , we arrive at an equation that expresses:

$$L = N_w w + N_B B \quad (4)$$

The values of the coefficients N_w and N_B for the two systems MQW and SQW may be defined as follows:

$$\begin{array}{ll} N_w = 1, & N_B = 0 & \text{for SQW} \\ N_B = N_w - 1 & & \text{for MQW} \end{array}$$

Well layer structure with homogenous cladding layers and the active layer's average thickness with average index refraction (\bar{n}_r) can achieve equation (5) [20].

$$\bar{n}_r = \frac{N_w w n_w + N_B B n_B}{L} \quad (5)$$

Use $\bar{\tau}$ instead of τ in equation (2) for the optical confinement factor of a MQW, which is given by:

$$\bar{\tau} = 2\pi \left(\frac{D}{\lambda}\right) \sqrt{\bar{n}_r^2 - n_c^2} \quad (6)$$

The confinement effects, which are in quantum wells, for example, are well-known quantum structures (QW), which appear in one dimension for quantum wells. At the same time, depending on the size of the confining region, the energy bands (conduction and valence) display separate instead of continuous energy bands as seen in bulk structures [21]:

$$U_i = \frac{(i\pi\hbar)^2}{2m^*w^2} \quad \text{for quantum well}$$

where i are principle quantum numbers ($i = 1, 2, 3, \dots$).

2.2. Recombination Coefficient

Radiative recombination happens when electrons in the conduction band combine with holes in the valence band, resulting in the emission of a photon. Radiative emission can occur naturally or as a result of a stimulus emitting a photon. Radiative emission may be from spontaneous emission or stimulated emission [22].

$$R_r = B_{\text{rad}} N^2 \quad (7)$$

The radiative recombination coefficient, where N is the carrier concentration and B_{rad} is the radiative recombination coefficient, may be represented as [23]

$$B_{\text{rad}} = \frac{e^2 w n_r E_g |M_{\text{ave}}|^2}{\epsilon_0 C^3 m_0^2 k_b T m_h^* (1+r)} \quad (8)$$

where e is the electron charge, m_0 is the free electron mass, E_g is the energy band gap, ϵ_0 is the vacuum permittivity, C is the light velocity, k_b is the Boltzmann constant, $r = m_e^*/m_h^*$, n_r is the refractive index, and $|M_{\text{ave}}|^2$ is the average of the squared momentum matrix element.

Auger recombination rate is expressed as [24].

$$R_{\text{Aug}} = (C_p + C_n)n^3 = C_{\text{Aug}}N^3 \quad (9)$$

C_p , C_n are the electron and hole Auger coefficients, respectively, while C_{Aug} is the Auger recombination coefficient, which may be expressed as [22].

$$C_{\text{Aug}} = \frac{1}{\tau_A N^2} = C_o \exp\left(\frac{-E_a}{k_b T}\right) \quad (10)$$

where τ_A is the lifetime of Auger carrier, C_o and E_a are the coefficient in the (CHCC) Auger process and activation energy.

3. Results and discussion

Well width (w), barrier width (B) and their effect on the optical confinement factor are important structure parameters that are calculated and simulated. The well material is InP for both single-quantum well and multi-quantum well structures. The active region of MQW consists of three, four, and five InP wells and two, three, and four InGaAsP barrier layers alternately, where InGaP is the cladding layer. Because of their usefulness in many technologies, multi-quantum wells are being studied. Equations (2) and (3) were used to obtain the optical confinement factor for SQW and MQW, respectively. Figure 1 shows (Γ) in relation to (w) and for different barrier widths. For each value of the barrier width (2nm, 6nm, 10nm, 14nm, and 18nm), the optical confinement factor rises with increasing well width. At a specific value of well width, the curves in Figure 1 intersect. For every value of barrier width, the optical confinement factor is unchanged at this value. However, for well widths less than a certain value, it appears that the rate of change in optical confinement factor when rising barrier width (B) may be ignored, but for barrier widths of 2 nm, the changing rate of optical confinement factor is greater than for other barriers above a certain value. The certain values of the optical confinement factor are 0.23, 0.216, and 0.203 for the number of wells 3, 4, 5, and well width (27, 19.5, and 15) nm, respectively (figure 1a, 1b, and 1c). This figure illustrates that the optical confinement factor for $N = 5$ is higher than $N = 3, 4$ for all barrier widths after a certain value. As for the variation of the confinement factor for the InGaAsP/InP QW structure with well width, it decreases as well width decreases. Because the quantized energy levels in QW lasers are dependent on well width, the photon energy output is a function of well width. The value of the well material's index of refraction is affected by this change in photon energy or wavelength. This research ignores variations in index of refraction as a function of the wavelength of radiated photons. The data is now unavailable due to a lack of interest in this material system. As a consequence, the index of refraction of the well material is adjusted to 3.4[25], that of the barrier layer to 3.28, and that of the cladding layer to 3.1. Consider a MQW structure like the one shown in the picture as a three-region waveguide with identical cladding layers and a well layer with an index of refraction and average thickness to find the confinement factor. [26].

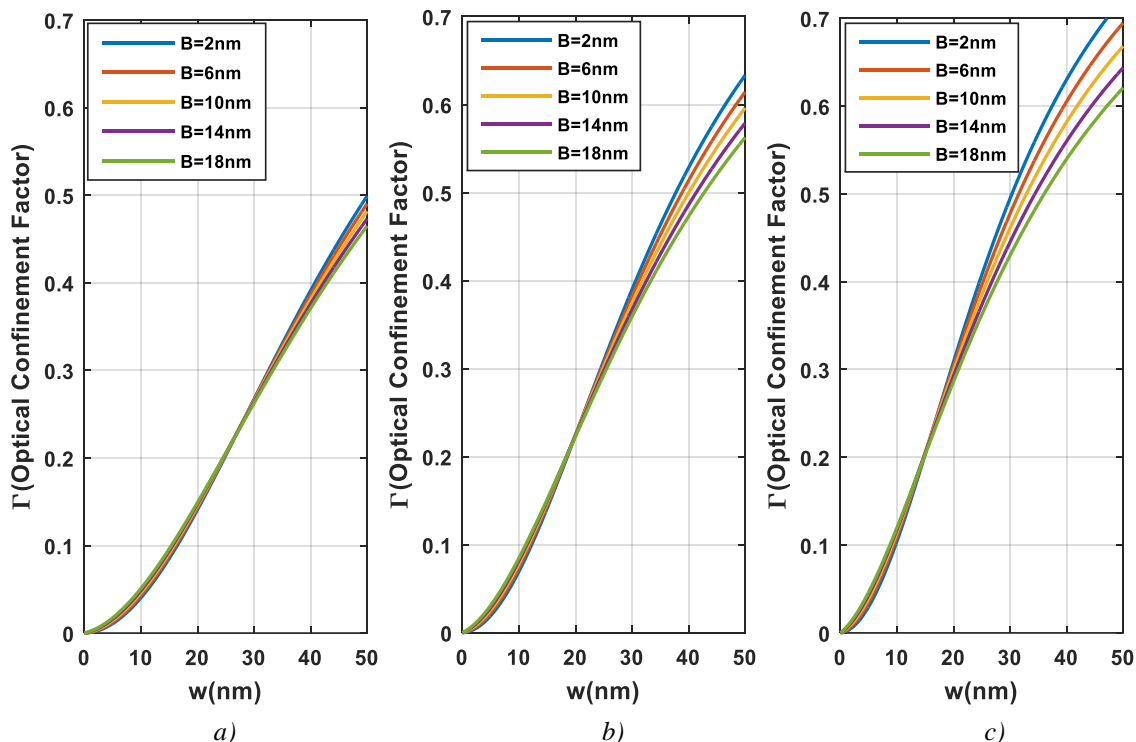


Fig. 1. The (Γ) in relation to (w) for variation barrier width of InGaAsP/InP MQWs.

When comparing a single quantum well to a multi-quantum well at $B = 2\text{ nm}$ for 3, 4, and 5 wells, Figure 2 demonstrates that the optical confinement factor for a single quantum well is very small for each value of well width. Because the optical confinement factor in a SQW is determined by the square well width (w^2), whereas the optical confinement factor in a multi-quantum well is determined by L . For narrower barrier well widths, however, for MQW design structures, the confinement factor values are larger and more sensitive to changes in thickness values.

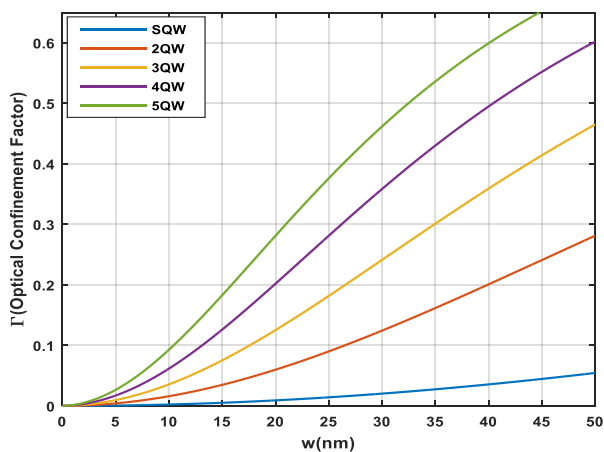


Fig. 2. The (Γ) in relation to (w) for InGaAsP/InP SQW and MQWs systems.

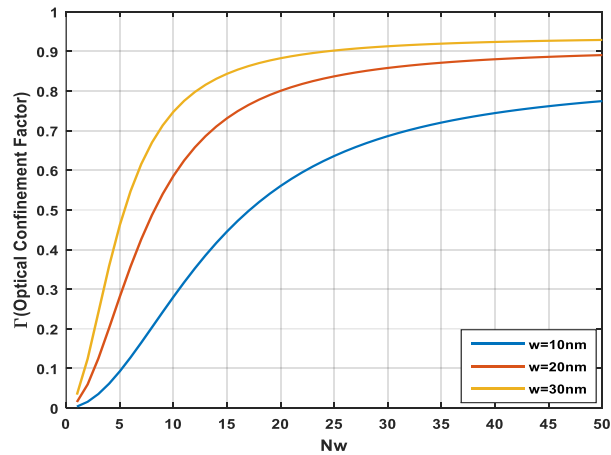


Fig. 3. The (Γ) as a function of (Nw) for InGaAsP/InP.

Figure 3 depicts the confinement factor in relation to the number of wells for multi-quantum well laser. The confinement factor in this figure grows as the number of wells grows. This figure was done for a well width (10, 20, and 30) nm and with a fixed 2 nm barrier thickness. The values of the confinement factor are, however, dependent on the barrier thickness through (4) and (5). As the barrier thickness grows, the confinement factor decreases, as demonstrated in the inset of Fig. 1. Barriers that are thinner fall faster than those that are thicker. As a result, using barrier thicknesses that match to well width values in a MQW reduces the confinement factor from $B = 2$ nm. As may be seen in the inset of Figure 1, increasing the thickness of the barrier has no effect on the confinement values. For thinner barriers, however, the confinement factor values for MQW design structures are more sensitive to changes and larger in thickness values.

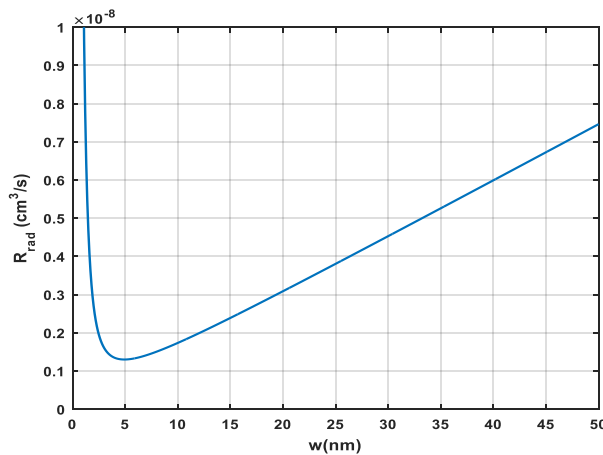


Fig. 4. Represents the relationship between the radiative recombination coefficient and the well width.

The radiative recombination coefficient was calculated from eq. (8) as shown in figure 4. We notice that the coefficient of the radiative recombination coefficient increases with increasing the width of the quantum well after 5 nanometers of well width. The increase is striking, and we note that the coefficient of radiative recombination in nano dimensions is 100 times greater than in the bulk. The increase in the radiative recombination coefficient when increasing the width of the quantum well is due to the increase in the number of carriers that are confinement in the well, which leads to an increase in the possibility of carrier combination.

The direct Auger recombination coefficient was calculated from eq. (10) as shown in figures 5 and 6. Auger recombination is a critical concern in mid-infrared devices because it is

band gap sensitive, rising as the semiconductor's band gap decreases. This is because when the band gap narrows, the effective mass of carriers and activation energy fall, causing the activation energy and effective mass of carriers to increase. By altering the band gap of diode lasers with temperature and hydrostatic pressure, the percentage contribution of non-radiative Auger recombination to the threshold current may be calculated experimentally. The band-to-band Auger process conserves momentum in an electron-hole transition without the need for phonons. The conservation of energy and momentum concepts explain why direct Auger operations are so reliant on band structure. Process energy is activated by maintaining extra momentum in direct Auger operations. The bandgap has a significant impact on the activation energy. There is no activation energy without momentum conservation. As a result, if the conservation of momentum is not proven, a significant dependence on the band structure will not be demonstrated. The phonon can conserve momentum in phonon-assisted Auger actions. As a result, in phonon-assisted Auger processes, we might expect the influence of the band structure to be less prominent.

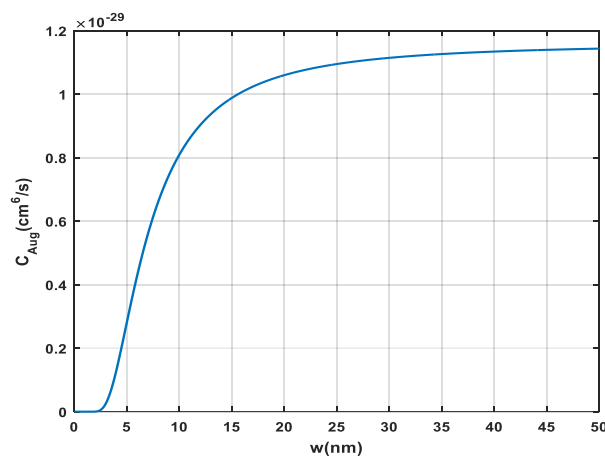


Fig. 5. Shows the relationship of the Auger coefficient with the width of the well.

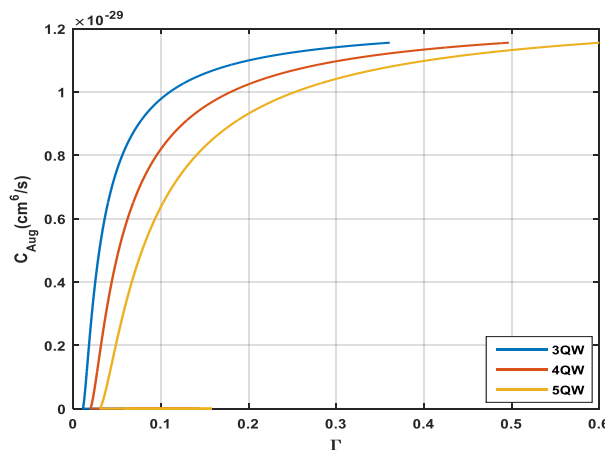


Fig. 6. The relationship of the Auger coefficient with the optical confinement factor.

We notice from these figures that the Auger coefficient decreases with the decrease in the width of the quantum well and decreases with the number of quantum wells, which indicates that the use of the number of quantum wells of 5 is better than 3 in a multi-quantum well system. From Figures 5 and 6, we note that the increase in the coefficient of radiative recombination is greater than the increase in the coefficient of Auger, and this indicates that at the nanoscale of the quantum well, the profit is achieved.

4. Conclusions

In conclusion, the InP Quantum Well laser structure emitted a wavelength of 924 nm in the IR range. The optical confinement factor of this structure increases as well number and well widths rise. It has a larger value when the barrier width is the smallest (2nm). For the InGaAsP/InP Quantum Well laser structure, the greatest value of the optical confinement factor is found at well number 5. In the single quantum well, the optical confinement factor is very tiny in comparison with the optical confinement factor in the multi quantum well for the same well and barrier width. The coefficient of radiative recombination increases by increasing the width of the quantum well after 5 nanometers. It is also larger than in the bulk structure. The coefficient of non-radiative recombination (Auger) decreases with the decrease in the width of the quantum well and increases the number of quantum wells. The Auger coefficient for the quantum well structure is less than that of the bulk structure. In this work, the preferred number of wells is 5.

References

- [1] J. V. Moloney, J. Hader, and W. Koch.Stephani, Laser Photon. Rev. 1,1, 24 (2007); <https://doi.org/10.1002/lpor.200610003>
- [2] M. R. Jobayr, E. M-T. Salman, and A. S. Kiteb, IHJPAS. 23,3, 95 (2017)
- [3] K. James Singh, T. Ahmed, P. Gautam, A. S. Sadhu, D. H. Lien, S. C. Chen, and H. C. Kuo, NanoMate. 11,6, 1549 (2021); <https://doi.org/10.3390/nano11061549>
- [4] M. R. Jobayr, and E. M-T. Salman, Chin. J. Phys. 74,270 (2021); <https://doi.org/10.1016/j.cjph.2021.07.041>
- [5] M. R. Jobayr, IHJPAS. 23, 1, 161 (2017); <https://doi.org/10.1016/j.surg.2016.06.063>
- [6] E. M-T. Salman, and W. K. Abad, Proc.3rd Fem. Sci. Conf. University of Baghdad. 7th-8th December (2016)
- [7] K. M. Qader, and E. M-T. Salman, Energy Procedia 157, 75 (2019); <https://doi.org/10.1016/j.egypro.2018.11.166>
- [8] F. Hadjaj, M. Belhadj, K. Laoufi, and A. Missoum, Journal of Ovonic Research, 17, 2, 107 (2021); https://chalcogen.ro/107_HadjajF.pdf
- [9] S. Tanaka, Y. Ogino, K. Yamada, T. Omori, R. Ogura, S. Teramura, and I. Akasaki, Appl. Phys. Lett. 118, 16, 163504 (2021); <https://doi.org/10.1063/5.0046224>
- [10] H. Jang, I. Karnadi, P. Pramudita, J. H. Song, K. Soo Kim, and Y. H. Lee, Appl. Phys. Lett. 6, 1, 1 (2015); <https://doi.org/10.1038/ncomms9276>
- [11] S. Khanna, and S. Nivedita, IJIRT 1, 6, 1659 (2014)
- [12] B. A. Ikyo, Am. J. Opt. Photon. 3, 5, 80 (2015)); <https://doi.org/10.11648/j.ajop.20150305.14>
- [13] J. H. Yang, L. Shi, L. W. Wang, and S. H. Wei, Scientific reports 6, 1, 1 (2016)
- [14] A. H. Kasim, and A. Makarimi, Threshold current temperature dependence of indium phosphide quantum dot lasers, Diss. Cardiff University, 2014
- [15] Z. Yin, and X. Tang, Solid-state electronics 51, 1, 6 (2007); <https://doi.org/10.1016/j.sse.2006.12.005>
- [16] A. A. Al-mfrji, NJES. 14, 2, 205 (2011)
- [17] W. K. Abad, Theoretical comparison between HgCdTe and AlGaAs Heterostructure Quantum Well laser Systems, University of Baghdad, 2015
- [18] M. Khodr, Nanoengineering: Fabrication, Properties, Optics, and Devices VI 7402, International Society for Optics and Photonics, (2009)
- [19] M. F. Khodr, P. J. McCann, and B. A. Mason, IEEE JQE. 34, 9, 1604 (1998); <https://doi.org/10.1109/3.709577>
- [20] N. R. Barai, and R. Basak, IJAREEIE 3, 8, 11047 (2014)
- [21] O. Manasreh, Semiconductor heterojunctions and nanostructures. McGraw-Hill, Inc., 2005

- [22] B. A. Ikyo, American Journal of Optics and Photonics 3, 5, 80 (2015);
<https://doi.org/10.11648/j.ajop.20150305.14>
- [23] B. Gönül, and M. Oduncuoğlu, Semi. Scie. Tech. 19, 1, 23 (2003)
- [24] H. Zhao, G. Liu, R. A. Arif, and N. Tansu, Solid-State Electronics 54,10, 1119 (2010);
<https://doi.org/10.1016/j.sse.2010.05.019>
- [25] B. R. Bennett, R. A. Soref, and J. A. Del Alamo, IEEE JQE 26, 1, 113 (1990);
<https://doi.org/10.1109/3.44924>
- [26] J. Guo, J. Tan, P. Hu, and S. T. Cundiff, Opt. Express 29,3, 3956 (2021);
<https://doi.org/10.1364/OE.414312>